EFFICIENT DYNAMIC MODELLING OF A TRICKLE BED REACTOR FOR DESULPHURISATION OF BIOGAS

N. Weiss[1], M. Harasek[2], M. Kozek[1]
[1]Inst. f. Mechanics and Mechatronics, Vienna Univ. of Technology, Austria
[2]Inst. f. Chemical Engineering, Vienna Univ. of Technology, Austria

Corresponding author: N. Weiss, Vienna Univ. of Technology, Inst. f. Mechanics and Mechatronics
1040 Wien, Wiedner Hauptstraße 8-10, Austria, nicole.weiss@student.tuwien.ac.at

Abstract. The main goal of this study was to develop a grey-box simulation model of the H_2S degradation process in a trickle bed reactor using physico-chemical models and experimental data. Measurements were taken at the biogas plant in Bruck/Leitha (40 km outside of Vienna) with a maximum biogas capacity of 1000 m^3/h. The structure of the model is based on the idea of an ideal local discretised plug flow reactor which performs like a stirred tank cascade with ten stages. Desulphurisation is done by microorganisms (*Thiobacillus thiooxidans*) which convert H_2S into elemental sulphur and sulphuric acid. The mass transfer between gas and liquid phase is accounted for by the two-film theory. The mass balances were implemented in a non-linear dynamic model in Matlab/Simulink. This model is validated against one series of measurements.

1 Introduction

Biogas is of great significance in the field of renewable energy while desulphurisation remains a major obstacle in the purification process. Trickle bed reactors working with microorganisms [1] are a standard state-of-the-art method to remove hydrogen sulphide H_2S. However, varying H_2S concentrations and gas flows have a negative impact on the removal efficiency if no process control measures are taken. Also, subsequent biogas upgrading requires keeping the output concentration of oxygen in the treated biogas below certain limits [2].
The goal of this study was to develop a grey-box model of the H_2S degradation process in a trickle bed reactor using physico-chemical models and experimental data. Measurements were taken at the biogas plant in Bruck-/Leitha (40 km outside of Vienna) with a maximum biogas capacity of 1000 m^3/h. The crude gas is fed into the reactor where H_2S is absorbed by the liquid phase with help of the packing material (grid-shaped HDPE objects). Desulphurisation is done by microorganisms (*Thiobacillus thiooxidans*) which convert H_2S into elemental sulphur and sulphuric acid [3, 4]. These bacteria need oxygen in order to oxidise sulphide to sulphate. O_2 is added to the crude gas before it enters the reactor. The liquid phase is recycled and returned into the reactor by counter current flow. Therefore, the dynamic model has three significant inputs and two outputs. The only actuating variable is the O_2 input concentration. The volume gas flow rate and the H_2S input concentration are disturbance variables. The H_2S and O_2 output concentrations are the output variables.
The remainder of the paper is structured as follows: In section 2 the modelling process is explained and the analytical as well as the experimental model parts are derived. The subsequent section shows simulation results for the full nonlinear model and demonstrates the versatility of the multi-input multi-output (MIMO) approach. In section 4 the experimental validation of the nonlinear model is performed by comparison with extensive measurement data from the plant. Furthermore, a section is dedicated to the linearisation of the model in order to design suitable controllers for the process. Some concluding remarks are given at the end.

2 Modelling

The structure of the mathematical model is based on the idea of an ideal local discretised plug flow reactor which performs like a stirred tank cascade with ten stages (elements), see Figure 4 (b). For wastewater treatment there exist similar ideas, but Wik [5] and Janssen et al. [6] put their emphasis on the chemical and biological processes in the liquid phase and the biofilm. Wik actually neglects the gas phase and Janssen et al. control the oxygen regulation by controlling the redox potential. On the contrary, Deshusses et al. [7] concentrate on the gas phase, but do not deal with desulphurisation and oxygen addition. In this paper a different approach is proposed, which is better suited for the investigation of biogas desulphurisation.

2.1 Flow Characteristics

Gas flow characteristics from CFD-simulations at reactor input and mass distribution in the reactor are represented in Figure 1. Figure 1 (a) clearly shows that the assumptions of a homogenous plug flow inside the reactor are fulfilled even at the very bottom. This effect has been achieved by a careful design of the gas feed to the reactor. Figure 1 (b) demonstrates the propagation of a step in input concentration to the top of the column. A strong gradient can be seen near the top (colour change from blue to red) which corresponds to the sigmoid transient which can also be seen in Figure 4 (a).

During stationary operation a constant and homogenous flow velocity exists, as can be seen at the bottom of the column. So the pressure drop along the vertical axes of the reactor is insignificant and therefore neglected. Furthermore, it is demonstrated that in each stage the concentrations are constant in radial direction.

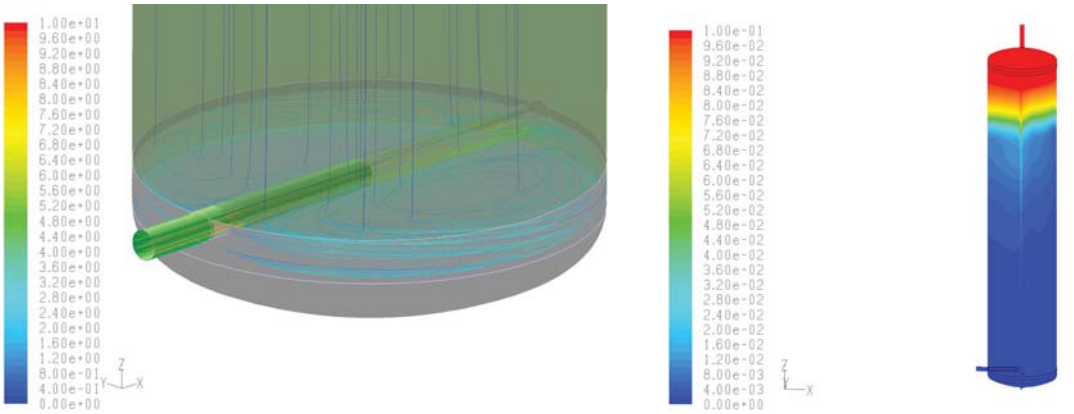

(a) Gas flow characteristics at reactor input in m/s

(b) Distribution of H_2S after step input in kg/m^3

Figure 1: Flow characteristics at reactor input and H_2S distribution after step input in the reactor (CFD-Simulation in FLUENT: with kind permission of Christian Jordan).

2.2 Mass Transfer and Mass Balance

The mass transfer between gas and liquid phase is accounted for by the two-film theory [8], see Figure 2 (a). This theory is based on the idea of two laminar boundary layers conterminous to the interface *Ph*. These layers are responsible for the resistance of the mass transfer from gas to liquid phase. In each laminar boundary layer the mass transfer described by the mass transfer coefficents β and β_l [m/s] is caused by molecular diffusion. At the interface itself a phase equilibrium can be observed. Beyond the laminar boundary layers the H_2S and O_2 concentrations are assumed to be constant in both gas and liquid phase because of turbulent convection. Sattler [8] and Mackoviak [9] specify mathematical correlations for the calculation of the total gas and liquid mass transfer coefficients k resp. k_l [m/s].

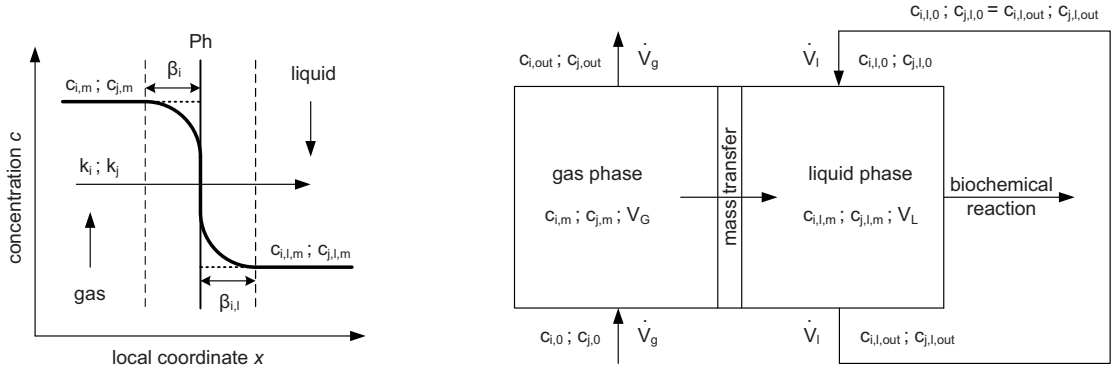

(a) Two-film theory

(b) Mass balance

Figure 2: Structure of two-film theory and mass balance. The chemical reaction kinetics are experimentally determined by parameter estimation.

The specific surface area a [m^2/m^3] of the packing material is known. V_G and V_L [m^3] describe the volumes of the gas and liquid phases of the single elements whereas $\dot{V}_g$ and $\dot{V}_l$ [m^3/s] are the gas and liquid volume flow. The equilibrium constant m [-] depends on the Henry coefficient. The reaction rate δ [s/(kg·m^3)] relies upon the activity of the bacteria and is experimentally determined by parameter estimation. For the model here proposed, this rate is assumed to be constant. The reaction mechanisms are represented in equation (1) and (2).

Direct oxidation:

$$H_2S + 2O_2 \xrightarrow{\text{microorganisms}} H_2SO_4 \tag{1}$$

Oxidation with elemental sulphur as intermediate:

$$2H_2S + O_2 \longrightarrow 2S + 2H_2O \tag{2}$$

$$2\,S + 2\,H_2O + 3\,O_2 \xrightarrow{\text{microorganisms}} 2\,H_2SO_4$$

The mass balance (Figure 2 b) of the gas phase for one single element is shown in the first differential equation (1). The concentrations of H_2S and O_2 (indices i and j respectively) are represented by c_n [kg/m^3] in the gas phase, whereas $c_{l,n}$ [kg/m^3] describes the concentrations in the liquid phase. The correct time delay (dead time $\tau = V_G/\dot{V}_g$ [s]) for $c_{i,n}$ and $c_{j,n}$ while passing each individual stage has to be considered.
Equation (3) is valid for both substances, $n = 1, 2, \ldots, 10$.

$$V_G \frac{dc_{i,n}(t)}{dt} = \underbrace{\dot{V}_g \left[c_{i,n-1}\overbrace{(t-\tau)}^{time\ delay} - c_{i,n}(t)\right]}_{input-output} - \underbrace{k_i \cdot a \cdot V_G \left[c_{i,n}(t) - c_{i,l,n}(t) \cdot m_i\right]}_{mass\ transfer} \tag{3}$$

The mass balance of the liquid phase is described in equation (4). Here again the dead time $\tau_l = V_L/\dot{V}_l$ [s] has to be considered. This equation is not valid for the substance O_2 because the microorganisms do not only consume O_2 to degrade H_2S, but also use it for other unknown degradation processes and for their basic metabolism. Therefore, an additional polynomial term is added, see equation (5). This black-box term is approximated using experimental data.

$$\begin{aligned} V_L \frac{dc_{i,l,n}(t)}{dt} &= \dot{V}_l \left[c_{i,l,n+1}(t-\tau_l) - c_{i,l,n}(t)\right] + k_i \cdot a \cdot V_G \left[c_{i,n}(t) - c_{i,l,n}(t) \cdot m_i\right] \\ &\quad \underbrace{- V_L \cdot c_{i,n}(t) \cdot c_{j,n}(t) \cdot \delta}_{reaction\ kinetics} \end{aligned} \tag{4}$$

$$\begin{aligned} V_L \frac{dc_{j,l,n}(t)}{dt} &= \dot{V}_l \left[c_{j,l,n+1}(t-\tau_l) - c_{j,l,n}(t)\right] + k_j \cdot a \cdot V_G \left[c_{j,n}(t) - c_{j,l,n}(t) \cdot m_j\right] \\ &\quad - V_L \cdot c_{i,n}(t) \cdot c_{j,n}(t) \cdot \delta \\ &\quad \underbrace{- V_L \cdot \left[d_4 \cdot c_{j,n}^4(t) + d_3 \cdot c_{j,n}^3(t) + d_2 \cdot c_{j,n}^2(t) + d_1 \cdot c_{j,n}(t) + d_0\right]}_{polynomial\ term} \end{aligned} \tag{5}$$

3 Simulation

The mass balances were implemented in a non-linear dynamic model in Matlab/Simulink, see Figure 3. In the table below the colour code of the simulink model is given. The equation terms are also designated in equations (3), (4) and (5). The Figure shows the structure of the differential equations of the first stage (subsystem 1). The other nine stages have the same structure.

colour	phase	substance	equation term
red	gas	H_2S, O_2	input, output
light blue	liquid	H_2S, O_2	input, output
dark blue	gas, liquid	H_2S, O_2	mass transfer
green	liquid	H_2S, O_2	reaction kinetics
grey	liquid	O_2	polynomial term
orange	gas, liquid	H_2S, O_2	time delay

Figure 4 shows some of the simulation results. At the beginning of the simulation the input concentrations are 2000 ppm H_2S and 0.75 % O_2 and the volume flow rate is 700 m^3/h. The figure shows the response of the model to two steps in the O_2 concentration and one step in the flow rate $\dot{V}_g$. In the table below the step times and amplitudes are given.

t	[s]	250	1000	2250
ΔO_2	[%]	-0.2	-	0.1
$\Delta \dot{V}_g$	[m^3/h]	-	-100	-

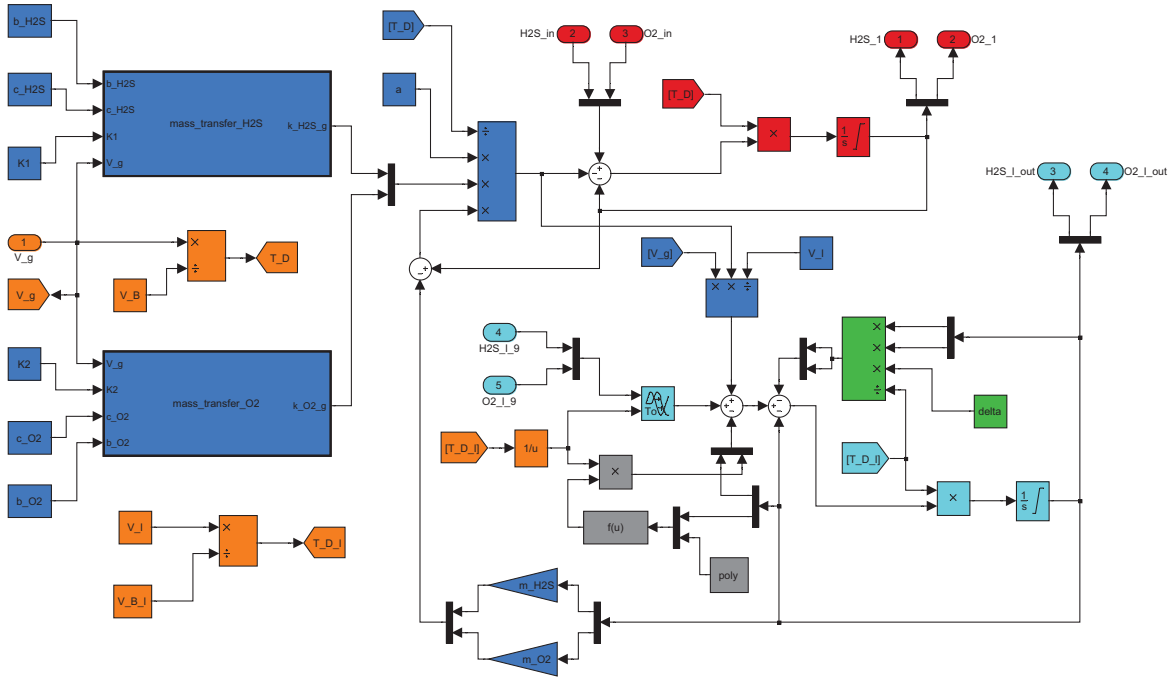

Figure 3: Non-linear model in Matlab/Simulink: Stage (Subsystem) 1

The first step of the O_2 concentration is negative, therefore the H_2S concentrations increase. The second step of the volume flow rate is also negative, but H_2S concentrations decrease. The last step of the O_2 concentration is positive, so H_2S concentrations decrease.
These step responses represent very clearly the dependence of the H_2S concentration on varying O_2 input concentrations and volume flow rate. Moreover, the importance of the dead time is shown, too. On O_2 input concentration steps the output reacts like a PT_n element with a cumulative dead-time which is typical for chemical plants while flow rate deviations cause a linear step response. This is due to the assumption of an ideal plug flow reactor.

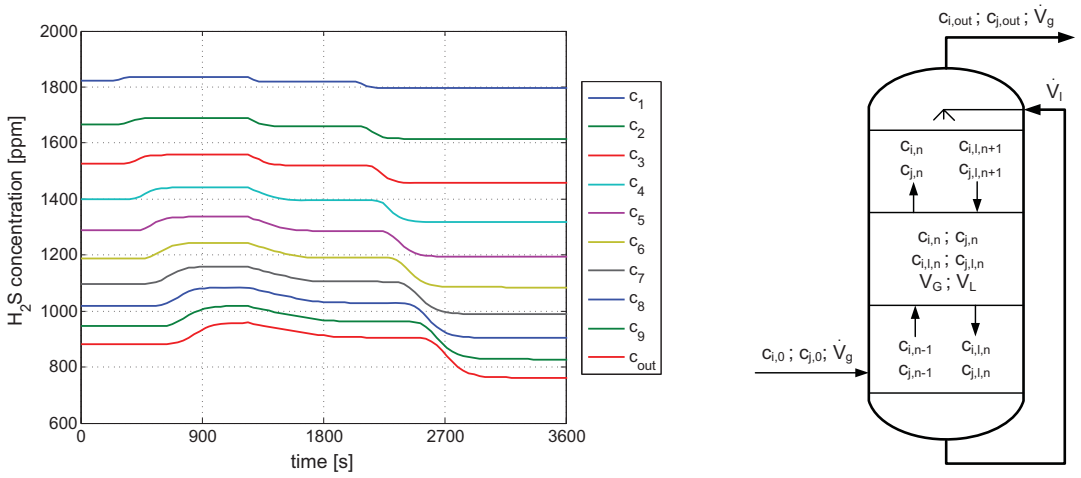

(a) Simulation results (b) Discretised plug flow reactor

Figure 4: Simulation results: step responses of the H_2S output concentration by varying the O_2 input concentration and the volume gas flow rate. Operating point: 2000 ppm H_2S, 0.75 % O_2, $\dot{V}_g = 700\ m^3/h$, first step at t = 250 s, $\Delta O_2 = -0.2$ %, second step at t = 2250 s, $\Delta \dot{V}_g = -100\ m^3/h$, third step at t = 2250 s, $\Delta O_2 = +0.1$ %

4 Experimental Validation

The model is validated against one series of measurements of 5 hours (Figure 5). The O_2 input and output concentration, the H_2S output concentration and the gas volume flow were recorded. The H_2S input concentration

was not explicitly measured, but can be derived from the stationary output concentration whenever the O_2 input concentration is zero. In the absence of O_2 the microorganisms are not able to metabolise any H_2S, hence under these circumstances input and output concentration have to be equal. The gas flow rate decreased from 710 to 610 and 455 m^3/h. The O_2 input concentration was increased from 0 to 0.8 % in steps of 0.1 %, and then decreased to 0.4 and 0 %. At the end it was set again to 0.4 and finally to 1.0 %.
The left diagram in Figure 5 shows the correlation between the simulated and the measured H_2S output concentration. The right one describes the same for the O_2 output concentration. At constant gas flow rates the model correlates with the measurements results. There are two sections (between 0.8-1.5 h and 2.9-3.2 h) where simulated and measured gas concentrations show significant deviations. This can be explained by very high flow rate gradients. They lead to dynamic effects which do not comply with the assumptions of the model structure. Moreover, the model does not account for deviations of the reaction rate which can differ at various H_2S or O_2 input concentrations, gas flow rates and temperatures.

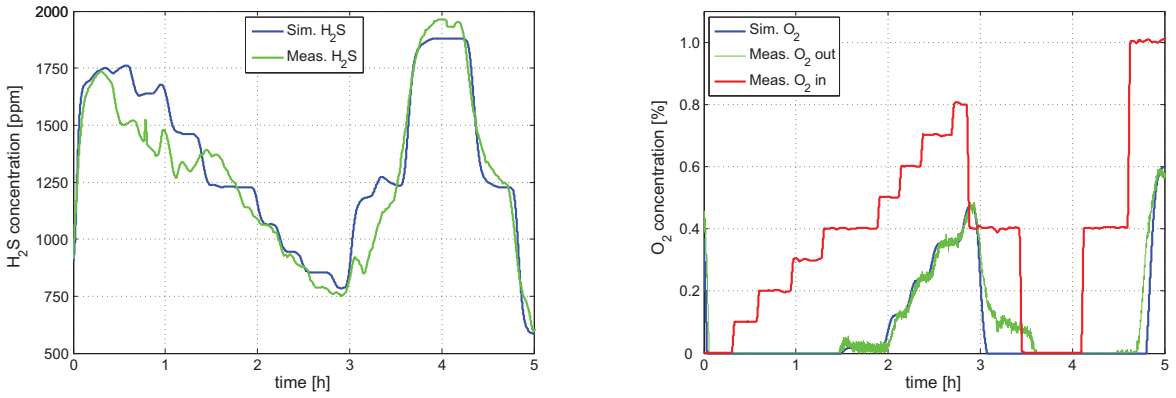

(a) (b)

Figure 5: Validation of the mathematical model: Correlation between simulated and measured output concentrations of H_2S and O_2. Operating point: H_2S input concentration is between 1750 and 1950 ppm, $\dot{V}_g$ decreases from 710 to 610 and 455 m^3/h and O_2 input concentration changes in steps.

5 Linearisation

The system dynamics of the non-linear mathematical model are identified by an output-error model [10]. Because of the multitude of time delays between the different stages and the counter current flow of gas and liquid phase, an analytical or numerical linearisation would require extensive Padè-Approximations or complex numerical methods. On the contrary, a black-box system identification with the output-error model yields fast and satisfactory results and is therefore chosen. The different tranfer functions from each input ($\dot{V}_g$, H_2S, O_2) to each output (H_2S, O_2) are generated by means of the Identification Toolbox in Matlab/Simulink.
The correlation between non-linear and linear simulation model is shown in Figure 6. The H_2S and O_2 input concentrations are 2000 ppm and 0.75 %. The volume flow rate $\dot{V}_g$ is kept constant at 700 m^3/h. Deviations from the operating point of O_2 input concentration lead to the step responses of the H_2S and O_2 output concentrations in diagram (a) and (b). In the table below the step times and amplitudes are given.

t	[s]	0	1600	3200	4800
ΔO_2	[%]	-0.1	0.2	-0.1	-0.2

It can be seen that the linear model of O_2 corresponds very well with the non-linear model. On the contrary, the linear model of H_2S shows larger deviations. This is due to the fact that the results of the generated tranfer function of O_2 input to H_2S output concentration differ from the measurement results. These differences are caused by the limited capabilities of the output-error model and by the more complex structure of the differential equation valid for O_2 liquid concentration.

6 Conclusion

The main goal of this study was to develop a grey-box simulation model of the H_2S degradation process in a trickle bed reactor using physico-chemical models and experimental data. The structure of the model is based on the idea of an ideal local discretised plug flow reactor which performs like a stirred tank cascade with ten stages. CFD-simulations in FLUENT show that the assumptions of an ideal plug flow inside the reactor are indeed fulfilled. Furthermore, the pressure drop along the vertical axes of the reactor is insignificant and neglected. The mass

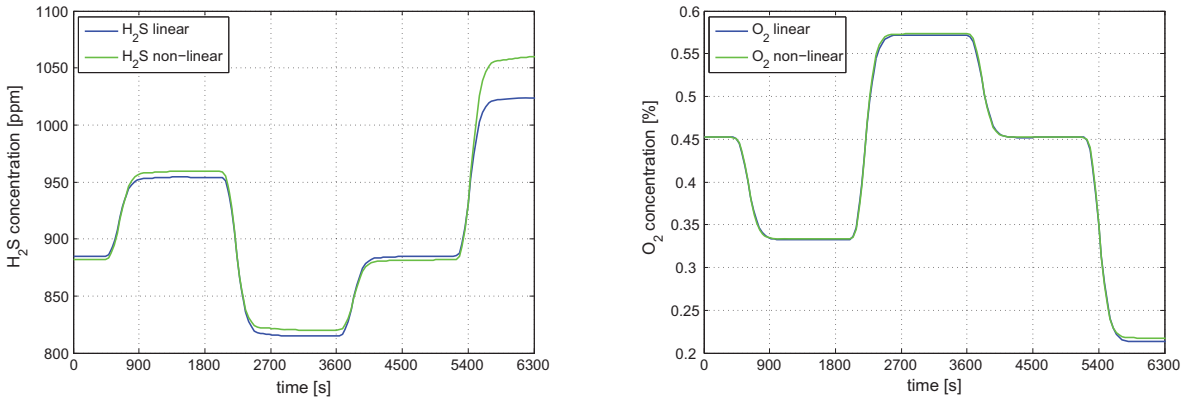

(a) (b)

Figure 6: Linearisation of the non-linear mathematical model: Correlation between linear and non-linear output concentrations of H_2S and O_2. Operating point: 2000 ppm H_2S, 0.75 % O_2, $\dot{V}_g = 700\,m^3/h$. O_2 input concentration changes in steps.

transfer between gas and liquid phase is accounted for by the two-film theory. By biochemical reactions H_2S is converted into elemental sulphur and sulphuric acid either by direct oxidation or by oxidation with elemental sulphur as intermediate. The reaction rate δ is assumed to be constant. Because of unknown degradation processes of the microorganisms, a black-box term approximated by experimental data is added to the mass balance of O_2 in the liquid phase. The mass balances were implemented in a nonlinear dynamic model in Matlab/Simulink. Simulation results show that on O_2 input concentration steps the output reacts like a PT_n element with a cumulative dead-time which is typical for chemical plants. Measurements were taken at the biogas plant. Hence, the model is validated against experimental data. At constant gas flow rates the model correlates well with the measurements results while at high flow rate gradients it lacks dynamic modelling of the flow and therefore leads to larger deviations. In order to design suitable controllers the model has been linearised. The system dynamic is identified by an output-error model which yields fast and satisfactory results.

Varying H_2S input concentrations and gas flows have a negative impact on the removal efficiency if no process control measures are taken. Also, subsequent biogas upgrading requires keeping the output concentration of oxygen in the treated biogas below certain limits. Further investigations are therefore recommended. Figure 7 (a) shows an example of a potential disturbance control. The simple but robust controller of the oxygen regulation is designed by the relations proposed by Chien-Hrones-Reswick. Figure 7 (b) shows the performance of the controlled non-linear system with and without disturbance compensation of H_2S and $\dot{V}_g$, respectively. It represents very clearly the advantages of a disturbance compensation of H_2S, but an additional measuring point for the H_2S input concentration is required. Moreover, if negative deviations from the operating point of the H_2S concentration occur, the controller will not kick in until certain limits are exceeded. An optimisation of the control design with an enhanced state space model would certainly improve the removal efficiency and ease the subsequent biogas upgrading.

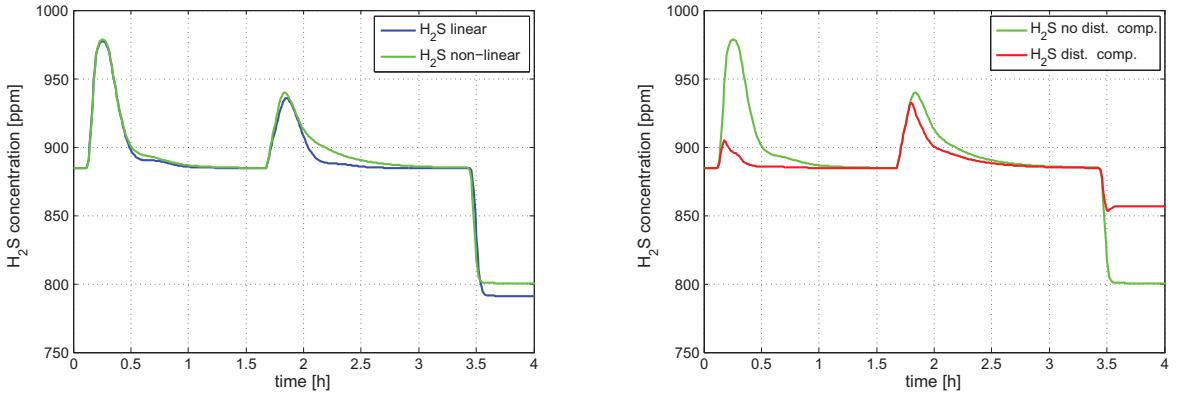

(a) (b)

Figure 7: Disturbance control: (a) Correlation between H_2S output concentrations of the controlled linear and non-linear system, no compensation. (b) Performance of the controlled non-linear system with and without disturbance compensation of H_2S and $\dot{V}_g$, respectively. Operating point: H_2S input concentration and $\dot{V}_g$ change in steps, O_2 input concentration is controlled.

7 References

[1] NN. Biologische Abgasreinigung, Biorieselbettreaktoren. VDI 3478 Blatt 2 Entwurf, 2005.

[2] NN. Natural Gas in Austria. ÖVGW Richtlinie G31, 2001.

[3] R. Forkmann and J. Hensel. Untersuchungen zur mikrobiologischen Entschwefelung von brennbaren Gasen mit hohen H_2S-Gehalten in Tropfkörperanlagen. In *Biologische Abgasreinigung - Gase, Gerüche, Keime*, VDI-Berichte 1777, pages 267–270. VDI Verlag, 2003.

[4] A. Janssen et al. Performance of a sulfide-oxidizing expanded-bed reactor supplied with dissolved oxygen. *Biotechnology and Bioengineering*, 53(1):32–40, 1997.

[5] T. Wik. Trickling filters and biofilm reactor modelling. *Reviews in Enviromental Science Biotechnology*, 2(2-4):193–212, 2003.

[6] A. Janssen et al. Application of the redox potential for controlling a sulphide oxidising bioreactor. *Biotechnology and Bioengineering*, 60(2):147–155, 1998.

[7] M. Deshusses et al. Behavior of biofilters of waste air biotreatment. 1. dynamic model development. *Enviromental Science Technology*, 29(4):1048–1058, 1995.

[8] K. Sattler. *Thermische Trennverfahren*. VCH, 1988.

[9] J. Mackowiak. Modellierung des flüssigseitigen Stoffüberganges in Kolonnen mit klassischen und gitterförmigen Füllkörpern. *Chemie Ingenieur Technik*, 80(1-2):57–77, 2008.

[10] L. Ljung. *System Identification: Theory for the User*. PRT Prentice Hall, 1999.